

Cristobalite inclusions in the Tatahouine achondrite: Implications for shock conditions

KARIM BENZERARA,^{1,*} FRANÇOIS GUYOT,¹ JEAN ALIX BARRAT,² PHILIPPE GILLET,³
AND MAURICE LESOURD⁴

¹Laboratoire de Minéralogie-Cristallographie, UMR 7590 and Institut de Physique du Globe de Paris, 4 place Jussieu, 75252 Paris Cedex, France

²Laboratoire de Géodynamique et Planétologie, UMR 6112 and Université d'Angers, Faculté des Sciences, 2 Bd Lavoisier, 49045 Angers Cedex, France

³Laboratoire de Sciences de la Terre, CNRS UMR 5570, Ecole Normale Supérieure de Lyon, 46 allée d'Italie, 69364 Lyon Cedex 07, France

⁴CNRS et Service Commun de Microscopie Electronique, Faculté de Médecine, Rue Haute de Reculée, 49045 Angers Cedex, France

ABSTRACT

The mineralogy of the Tatahouine diogenite was investigated by optical microscopy, Raman micro-spectrometry, and scanning and transmission electron microscopies. Inclusions of α -cristobalite in orthopyroxenes, locally in symplectic association with chromites, or associated with metal, have been characterized for the first time in a diogenite. Mosaicism of the orthopyroxenes indicates shock effects in the meteorite. The shock history of the meteorite must be consistent with the presence of vein-like structures containing inclusions of well-crystallized cristobalite, a low-pressure, high-temperature phase. Several possible mechanisms to account for these observations are discussed. The simplest one, consistent with all observations, is that a shock event would have occurred in a hot orthopyroxenite, either before extensive cooling of the asteroid, or in materials heated by previous impacts and maintained hot under an ejecta blanket.

INTRODUCTION

The fall of the Tatahouine meteorite was observed in 1931 (Lacroix 1931). It has recently attracted attention due to the presence of terrestrial nanobacteria associated with carbonates (Barrat et al. 1998; Barrat et al. 1999; Gillet et al. 2000a). This meteorite was classified as a diogenite based on mineralogical (Lacroix 1932) and isotopic (Clayton and Mayeda 1996) arguments. Diogenites are orthopyroxenite cumulates believed to have originated from asteroid 4-Vesta during an extensive magmatic event at 4.6 b.y. (e.g., Drake 1979; Binzel and Xu 1993; Warren 1997; Lugmair and Shukolyukov 1998). Only 25 such meteorites have been identified to date. Such objects provide unique observations of magmatic and impact events in the early solar system and thus deserve careful investigation.

Orthopyroxene has been widely investigated in Tatahouine (e.g., Lacroix 1932; Mittlefehldt 1994). Because reactions due to shock occurred after the magmatic processes ceased, the characterization of other constituent phases could help to determine the shock conditions of the meteorite. A study of accessory minerals that formed in situ in Tatahouine, is thus needed to obtain more precise information on the thermal history of the meteorite, as some minerals are better markers of pressure and temperature conditions than orthopyroxene. In this paper, we present a mineralogical study of new mineralogical characteristics of the Tatahouine diogenite.

EXPERIMENTAL TECHNIQUES

Polished thin slices of the Tatahouine meteorite were prepared from a hand specimen of the Tatahouine meteorite collected in 1994 by A. Carion. Additional petrographic observations documenting mosaicism in orthopyroxenes were performed on petrographic thin sections of the meteorite (sample no. 1643) supplied by the Museum National d'Histoire Naturelle de Paris.

For the scanning electron microscope (SEM) observations and X-ray energy dispersive spectrometry (EDS) chemical analyses, thin sections were carbon-coated using a Baltec modular high-vacuum coating system MED020. Operating conditions of the JEOL JSM6301-F microscope were 20 kV accelerating voltage and a sample-to-objective working distance of about 15 mm.

Transmission electron microscopy (TEM) samples were prepared from petrographic thin sections of orthopyroxene crystals displaying mosaicism (see below). Several petrographic thin slides removed from the sections were mounted on Cu grids, then thinned by an argon-ion beam in a Gatan PIPS ion mill operated at 3 kV and 10° on each gun, and finally coated with a thin film of carbon to prevent charging. The samples were studied with a JEOL 2000 EX transmission electron microscope operating at 200 kV and equipped with a Tracor-Northern TN 5400 FX energy-dispersive X-ray analyzer. EDS analyses were obtained in scanning transmission mode with a relatively large probe of about 100 nm.

* E-mail: benzerar@lmcp.jussieu.fr

Micro Raman spectra were recorded with a Dilor XY spectrometer equipped with confocal optics and a nitrogen-cooled CCD detector. A microscope was used to focus the excitation laser beam (514 nm exciting the line of a Spectra Physics Ar⁺ laser) to a 5 μm spot and to collect the Raman signal in the backscattered direction. Accumulations lasting from 120 to 300 seconds were made. The laser power on the sample was very small, from 2 to 50 mW, to avoid heat absorption and transformation of the minerals (Gillet et al. 2000b).

MINERALOGICAL OBSERVATIONS

According to previous descriptions (e.g., Lacroix 1931, 1932; Gooley and Moore 1976; Barrat et al. 1999), the Tatahouine diogenite is a green to light olive-gray shocked orthopyroxenite, consisting mostly of unbrecciated orthopyroxene crystals with fractures and dark bands (up to 2 mm wide) running through the material. Its texture is similar to that of some terrestrial igneous cumulates (adcumulates). The sizes of the pyroxene crystals are exceptional. Most of them are larger than 5 mm, and some crystals (locally subhedral) can reach 2 cm. Thin chromite patches (<3 mm in diameter) are commonly observed on clast surfaces. These patches were erroneously identified as “melted orthopyroxene” by Lacroix (1931, 1932).

Most orthopyroxene crystals have a mosaic appearance at extinction under a polarizing microscope (Fig. 1). Diagnostic criteria for the identification of this feature were presented by Stöffler et al. (1991) and are systematically observed in the Tatahouine meteorite. The single crystals display numerous domains that differ from each other in their extinction positions by more than 3°. Several crystals no longer exhibit a position of maximum extinction. Indeed, the mosaic domains (<1 μm in size) being smaller than the thickness of the thin section, are superimposed. Although Stöffler et al. (1991) noticed that the intensity of mosaicism is difficult to quantify optically in thin sections, we notice that the strong average misorientation

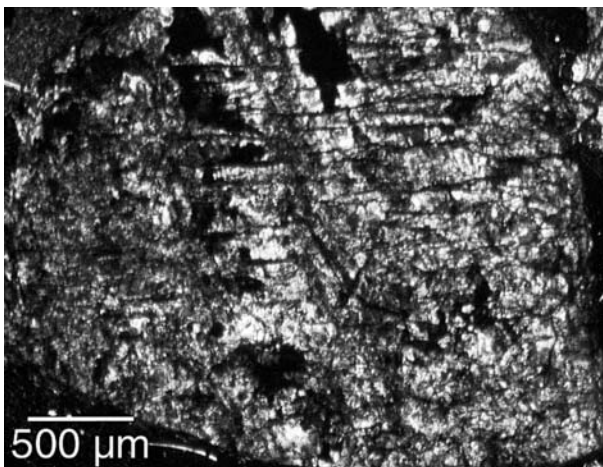


FIGURE 1. Optical micrograph showing planar fractures and the strong mosaicism in a Tatahouine orthopyroxene single crystal. Transmitted light, crossed polars. Some areas still assume an extinction position, whereas the major part of this single crystal shows a distinctly mottled appearance with no extinction position.

between domains and the small size of the different domains that we observe in Tatahouine are of the same order-of-magnitude as that observed in the strongly shocked meteorite Alfianello (shock stage S5, Rubin et al. 1997). This suggests that the mosaicism in Tatahouine can be considered as strong.

The compositions of the pyroxenes are uniform and cluster around $\text{Wo}_{1.5}\text{En}_{75.0}\text{Fs}_{23.5}$ (Fredriksson et al. 1976; Mittlefehldt 1994; Fowler et al. 1994; Barrat et al. 1999). The 18 Å spacing of the (100) planes (see the electron diffraction pattern in Fig. 2) confirms that the Tatahouine pyroxene is mainly the orthorhombic polymorph. Planar defects on (100) with heterogeneous distribution among different grains can be observed by TEM (Fig. 2) and have been previously documented by Nord and Hewins (1983). Similar defects have been studied extensively in pyroxenes by TEM (e.g., Buseck et al. 1980; Doukhan et al. 1986) and correspond to lamellae of clinopyroxene ($P2_1/c$). Densities of lamellae were found to be as high as 70 lamellae/ μm in some grains (Fig. 2), whereas they are missing in other grains.

Various types of inclusions in orthopyroxene crystals were

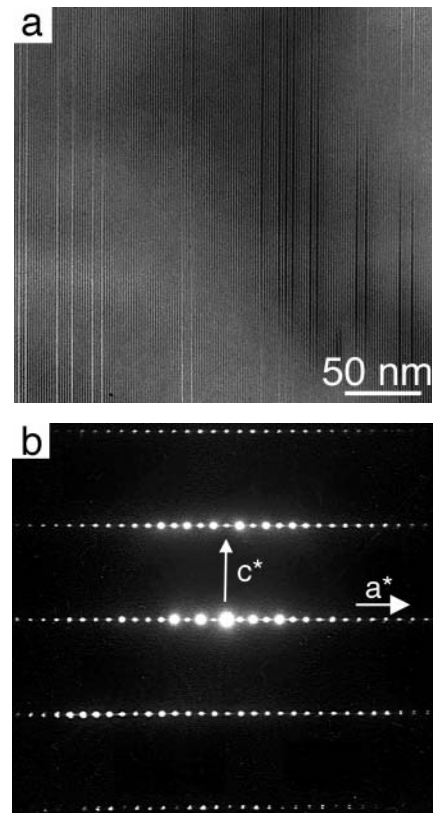


FIGURE 2. (a) Transmission electron microscope image of the Tatahouine orthopyroxene ([010] zone axis) containing putative clinopyroxene lamellae. Lattice fringes are parallel to (100). 18 Å repeats correspond to orthopyroxene. (b) SAED pattern of the same area in the same orientation. Notice the streaking in the $[100]^*$ induced by the high density of clinoenstatite lamellae. This pattern together with other patterns collected is consistent with orthopyroxene (space group $Pbca$, $a = 18.2 \text{ \AA}$, $b = 8.8 \text{ \AA}$, $c = 5.2 \text{ \AA}$).

identified by SEM backscattered electron (BSE) imaging (Fig. 3). They were previously described as “glassy inclusions” by Lacroix (1931, 1932). The most abundant are single-phase and composed of silica. Other inclusions are composite and may contain silica, chromite, metal (Fe 98%, Ni + Co 2%), and troilite in any combination. Silica and chromite locally form symplectitic intergrowths (Fig. 4). All the inclusions (<6% of the volume) are either elongated or resemble aligned droplets (Fig. 3), arranged in non-crystallographic planar arrays. They do not appear to define the borders of former anhedral pyroxene grains and no specifically high densities of inclusions can be observed near the margins of pyroxene crystals. In all cases, the silica phase was characterized by both micro-Raman spectroscopy (Fig. 5) and TEM (Fig. 6) and corresponds to well-crystallized cristobalite.

Because the silica inclusions embedded in orthopyroxenes are small, it is important to identify in the Raman spectra the vibrational bands of silica that would overlap with those of the orthopyroxene. We have thus recorded the Raman spectra of orthopyroxene in zones where this mineral was optically pure

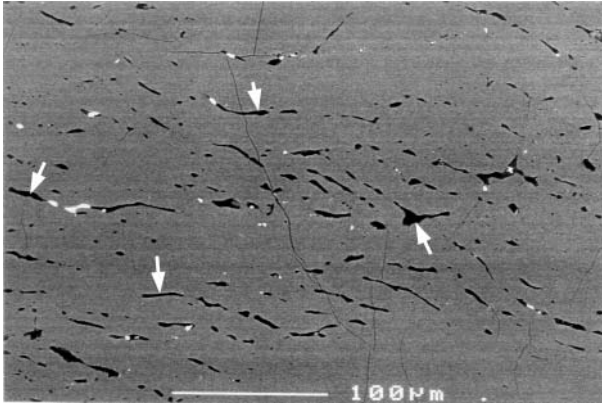


FIGURE 3. Backscattered electron image showing inclusions elongated along two major directions in the orthopyroxene host (gray). Dark silica inclusions (arrow) are numerous and associated with bright chromite and/or metal inclusions.

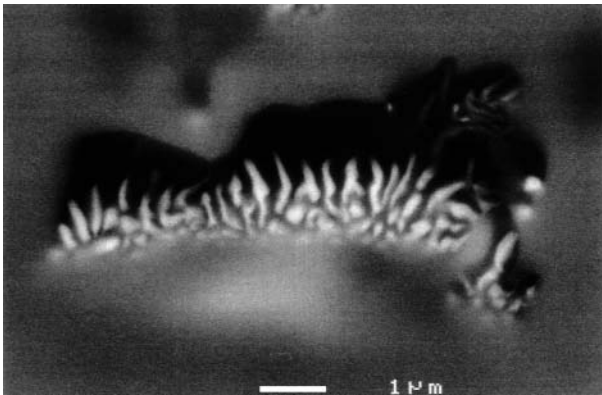


FIGURE 4. Backscattered electron image showing a symplectitic association of finely intergrown silica (dark) and chromite (light). The area of symplectitic association is embedded in orthopyroxene (gray).

enough to avoid contamination by other minerals (Fig. 5a). The Raman spectra of the silica inclusions (Fig. 5b) are characteristic of cristobalite (Palmer et al. 1994) and cannot be attributed to quartz, coesite, tridymite, or stishovite. The strong bands at 112, 228, and 417 cm^{-1} are unambiguously attributed to cristobalite (Fig. 5b).

The numerous electron diffraction patterns of the inclusions were also indexed unambiguously as α -cristobalite. As cristobalite was identified prior to and after TEM preparation, it cannot be the result of an artifact due to ion milling or beam damage. All the investigated inclusions display (101) planar defects (Fig. 6). The same defects were previously observed in α -cristobalites from low-pressure environments (e.g., Withers et al. 1989), but also in shocked materials (Martinez et al. 1993).

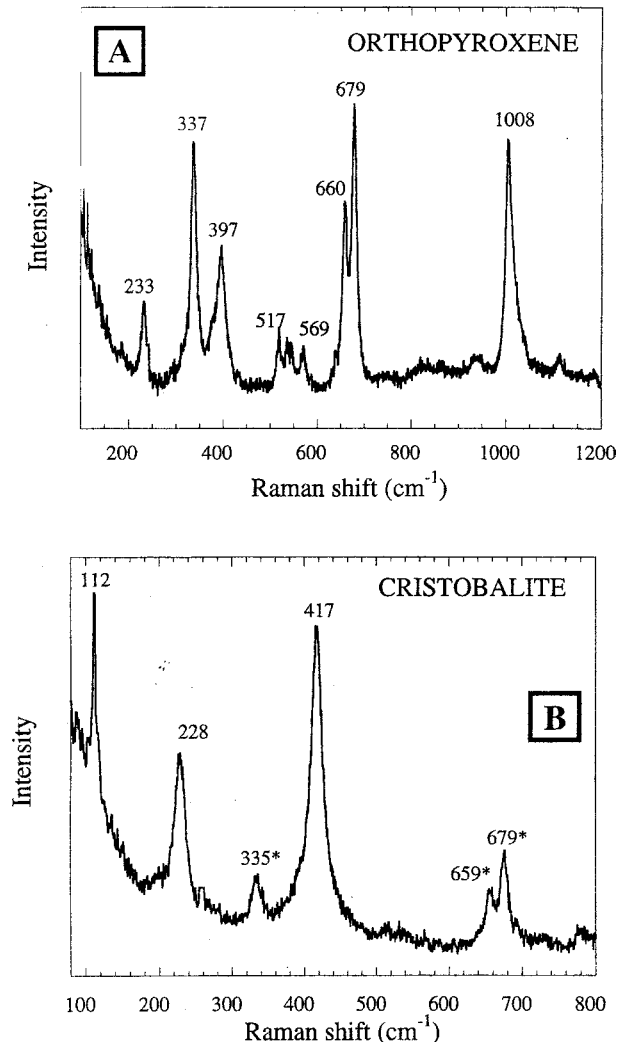


FIGURE 5. Raman spectra of orthopyroxene and cristobalite from the Tatahouine meteorite. Spectrum A was recorded far from any silica inclusion. All the peaks are characteristic of orthopyroxene (Sharma 1989). Spectrum B was obtained on a silica inclusion. The peaks at 112, 228, and 417 cm^{-1} are unambiguously attributed to cristobalite. Weak peaks (*) due to orthopyroxene surrounding the inclusion are still present (see spectrum A).

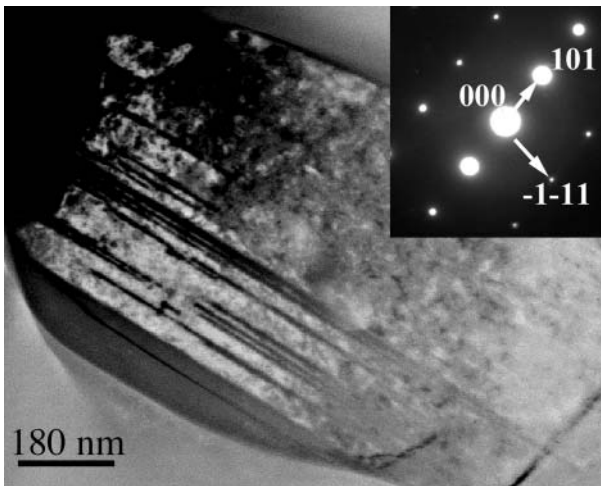


FIGURE 6. (a) TEM bright-field image of a α -cristobalite inclusion showing planar defects along (101). (b) Diffraction pattern; $d_{101} = 4.04$ Å; $d_{\bar{1}\bar{1}\bar{1}} = 3.13$ Å; angle between (101) and ($\bar{1}\bar{1}\bar{1}$) is 104° . This pattern together with other patterns collected is consistent with cristobalite (space group $P4_21_2$, $a = b = 4.97$ Å, $c = 6.92$ Å).

DISCUSSION

The α -cristobalite phase results from the inversion of β -cristobalite at about 250°C . Inversion of β -cristobalite into α -cristobalite results in numerous (101) planar defects (Withers et al. 1989), such as those observed in the present study (Fig. 6). β -cristobalite is stable between 1470 and 1728°C at a pressure of 1 atm (Frondel 1962). However, β -cristobalite can form metastably at lower temperature by heating glass, tridymite, or coesite (Rehfeldt et al. 1986; Gillet et al. 1990) at temperatures exceeding 1200°C . Some lower temperatures might even be invoked for cristobalite formation: Tsuchida and Yagi (1990) have reported that cristobalite submitted to pressures exceeding 35 GPa transforms into phase XI that transforms back into cristobalite upon pressure release under ambient temperature. Moreover, El Goresy et al. (2000) proposed that the cristobalites observed by TEM in the Shergotty meteorite resulted from the transformation of post-stishovite phases during ion-milling and electron irradiation. In the Tatahouine meteorite, however, cristobalite was observed by Raman spectroscopy prior to ion-milling preparation. If cristobalite had formed at relatively low temperature by quenching of a high-pressure silica polymorph, it would likely have produced a mixture of phases such as those reported by El Goresy et al. (2000), and this is not the case. Finally, it should be noted that in shock experiments, cristobalite, a low-pressure, high-temperature phase, is obviously not a common product and has difficulties surviving shock metamorphism. Gratz et al. (1993) have shown that cristobalite submitted to shock pressures higher than 23 GPa loses its crystallinity. It is therefore of interest to understand why free silica is present in the form of cristobalite in the Tatahouine meteorite, and how its presence is consistent with indications of strong shock metamorphism provided mostly by mosaicism in orthopyroxenes.

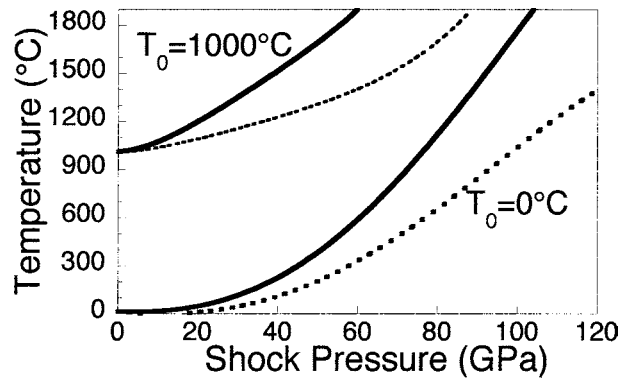


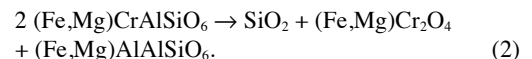
FIGURE 7. Calculated peak-shock (solid lines) and post-shock temperatures (dotted lines) plotted against the shock pressure for two initial temperatures ($T_0 = 0^\circ\text{C}$ for the two lower curves, $T_0 = 1000^\circ\text{C}$ for the two upper curves).

Origin of silica inclusions in Tatahouine

A silica polymorph, usually tridymite, is commonly observed in Howardites-Eucrites-Diogenites (HED) meteorites. For example, silica has been observed in the unshocked diogenite GRO95555 (Papike et al. 2000), and magmatic chromite/silica associations were described in Moama, a cumulate eucrite (Lovering 1975). A magmatic origin could thus be proposed for the cristobalite inclusions in the Tatahouine orthopyroxenes. However, the commonly observed associations of silica with chromite, Fe metal or Fe sulfide suggest that silica originated from post-magmatic thermal destabilization of pyroxenes, according to several reactions suggested previously (e.g., Brett 1976; Palme et al. 1988; Papike et al. 1995). For example, the formation of excess silica could have resulted from the reduction of Fe from pyroxene according to:



or by the destabilization of Cr-rich pyroxene according to:



In the present study, we do not observe gradients of Fe or Cr contents in pyroxene that could substantiate reactions 1 or 2, but such gradients might have been erased by subsequent thermal annealing. Cristobalite-chromite symplectites, such as those observed in Tatahouine (Fig. 4), have not been described in either extraterrestrial or terrestrial orthopyroxenes. Similar symplectitic textures consisting of magnetite and pyroxene have already been observed as inclusions in terrestrial and extraterrestrial olivines. The formation of these symplectitic lamellae has been a subject of debate but it has been shown that a high temperature ($>900^\circ\text{C}$) and a slow cooling process are required (e.g., Kondoh et al. 1985; Champness 1970; Greshake et al. 1998). The term symplectite is, however, of no genetic significance and the conditions for the formation of cristobalite-

chromite symplectites in the Tatahouine meteorite are thus unknown. Indeed, Gooley and Moore (1976) and Nord and Hewins (1983) have previously described the occurrence of metal, troilite, chromite, and silica inclusions associated in non-crystallographic planar arrays in the Tatahouine meteorite (Fig. 3) and have interpreted them as the result of metamorphism. In that sense, metamorphism could either be due to the thermal evolution of the parent body or to shock events.

The fact that many of the cristobalite inclusions occur without apparent associations with other phases should not be taken as a proof for a magmatic origin and as a point against post-magmatic metamorphism. Indeed, pyroxenes annealed at high temperatures but below their melting point have been reported to exsolve tiny precipitates of either pure silica or a molten phase enriched in silica (Doukhan et al. 1993).

In summary, cristobalite inclusions observed in the Tatahouine orthopyroxenes could be of magmatic or of high-temperature metamorphic origin (parent body thermal history or shock). Their relationship to the shock event that produced mosaicism observed in the orthopyroxenes is not clear and is discussed below.

Shock markers and shock-conditions

The classification of shock stages in enstatite chondrites (Rubin et al. 1997) provides a way of estimating shock pressures in these meteorites by optical microscopy. This classification is of special interest to the present study because it focuses on shock effects in orthopyroxenes. The strong mosaicism displayed by the orthopyroxene, the absence of (Mg-Fe) majorite, and the absence of evidence for melting in Tatahouine are typical of shock stage S5 (Rubin et al. 1997), suggesting that the shock pressure was in the range 25–60 GPa. The lamellae of clinopyroxene observed in the Tatahouine orthopyroxene may have formed under shock, although they could result from other processes (e.g., simple cooling). Surprisingly, in this study, the observed pyroxene grains that exhibit a strong mosaicism and are thus representative of shock stage 5, do not contain very high densities of clinopyroxene lamellae (Fig. 2), and those are barely visible optically. There appears to be some discrepancy between two shock indicators: the strong mosaicism and the low density of the clinopyroxene lamellae. Coe and Kirby (1975) demonstrated that clinoenstatite lamellae are removed by heating of orthopyroxene. One could speculate that most lamellae generated by the shock event in Tatahouine have been annealed by elevated post-shock temperatures. In that case, some or most of the observed lamellae could be of a different origin than shock. Metamorphism with heterogeneous temperature conditions such as shock metamorphism could additionally explain the heterogeneous density of lamellae observed among different grains of pyroxene, as suggested by Rubin et al. (1997). Nord and Hewins (1983) have previously noted the heterogeneous density of lamellae in the Tatahouine meteorite and had interpreted it as the result of post-shock thermal annealing.

In a quasi-monomineralic assemblage such as the Tatahouine orthopyroxenite, the relationship between shock pressures and temperatures depends mainly on the initial porosity and on the initial (pre-shock) temperature. In an orthopyroxenite cumu-

late, however, porosity is negligible. Shock temperatures can be estimated by integrating the following equation (e.g., Stöffler 1982):

$$\frac{dT}{dV} = -T \left(\frac{\gamma}{V} \right) + \frac{1}{2C_V} \left[(V_0 - V) \frac{dP}{dV} + (P - P_0) \right] \quad (3)$$

in which P is the pressure and V the specific volume (index 0 stands for initial values); T is the temperature along the Hugoniot, γ is the Grüneisen parameter (taken as a constant value), and C_V is the molar heat capacity. Then, the post-shock temperature is obtained by adiabatic decompression to 1 bar. Using the Hugoniot equation of state data of the Bushveld pyroxenite compiled in Stöffler (1982), and the specific heat of enstatite at 1 bar (Thiéblot et al. 1999), the relationship between peak-shock temperature, post-shock temperature, and shock pressure (considering two pre-shock temperatures of 0 and 1000 °C, respectively) is given in Figure 7. Sensitivity to various parameters has been tested by using different measured Hugoniot curves (of Stillwater pyroxenite, Bamble enstatite, and Bushveld pyroxenite; compiled in Stöffler 1982). Grüneisen parameters and specific heat were systematically varied within 20%, which encompass the maximum P and T effects on these parameters while integrating Equation 2. Whatever the variation of the different parameters, temperature estimations at a given pressure are of the same magnitude. A simpler method for calculating the post-shock temperature, in principle less exact, based on evaluation of shock residual energies (Gibbons and Ahrens 1971) has also been used for control, and has given consistent results.

In shock experiments, quartz and cristobalite completely amorphize for peak-pressures exceeding 35–40 GPa and 25 GPa, respectively (Zhang and Ong 1993; Gratz et al. 1993; Richet and Gillet 1997). Moreover, the shock amorphization of cristobalite begins at 23 GPa, as shown by a lowering of the refractive index (Gratz et al. 1993). Four possibilities are thus consistent with the observation of well-crystallized cristobalites in the Tatahouine meteorite:

(1) Cristobalite formation pre-dated the shock event and the intensity of the shock event was too low to induce amorphization (i.e., $P_{\text{shock}} < 23$ GPa; $T_{\text{shock}} < 80$ °C, $T_{\text{postshock}} < 30$ °C). The strong mosaicism displayed by the orthopyroxene, however, suggests shock pressures higher than 25 GPa (Rubin et al. 1997).

(2) Another possibility is a metastable, post-shock formation of cristobalite during a low-pressure and moderate temperature post-shock stage. The shock pressure range deduced from the shock classification implies a post-shock temperature range of 35–340 °C (Fig. 7). However, the formation of pure and well-crystallized cristobalite at such low temperatures has never been reported, although the possible role of back-transformation of post-stishovite, high-pressure phases deserves further investigation.

(3) A third possibility is that cristobalite formed immediately after the shock during a low-pressure and high-temperature (i.e., >1200 °C) post-shock stage. In that case, very high post-shock temperatures would be required to form well-crystallized cristobalite according to well-documented mechanisms.

To achieve postshock temperatures at zero pressure exceeding 1200 °C, unrealistically high shock pressures (>105 GPa) are needed. It would thus be necessary to invoke highly localized high temperatures, due to frictional heating, as proposed in Bischoff and Stöfler (1992), Chen and El Goresy (2000), and Malavergne et al. (2001). The occurrence of cristobalite in the Zagami meteorite has been interpreted in this way (Weber et al. 2000). However, no clear association of the cristobalite distribution in Tatahouine with either crystal defects in the orthopyroxenes or grain boundaries marking previous fractures has been observed.

(4) Finally, it could be proposed that the occurrence of a relatively low-pressure impact in hot orthopyroxenite could help to reconcile the intuition of Lacroix (1931, 1932) that the shock in Tatahouine was associated with textures of partial melting with relatively low shock pressures, consistent with the absence of high-pressure polymorphs of pyroxenes. Indeed, a low-pressure shock event (e.g., 35 GPa) in hot orthopyroxenite (an initial temperature of at least 1000 °C is required to reach the temperature of cristobalite formation during the post-shock stage in a 35 GPa shock, see Fig. 7) could make reactions 1 and 2 occur without leading to compositional zoning due to the high post-shock temperatures. Moreover, a low-pressure shock event could produce crystallization of cristobalites by mechanisms such as that proposed or re-crystallization of pre-existing cristobalites, and could possibly result in quite strong mosaicism in orthopyroxenes. Shock-wave experiments on preheated samples would be required to evaluate those possibilities, specifically whether formation of subgrain boundaries can lead to mosaicism and whether appropriate densities of lamellae form upon post-shock cooling. Indeed, the shock metamorphism of initially hot orthopyroxenes would not be unrealistic because a high initial temperature could have been achieved if the material was heated below an ejecta blanket, resulting from previous impact(s) (Palme et al. 1988). Alternatively, the impact could have occurred early after the differentiation of the HED parent body. The cooling duration of 4-Vesta, the putative parent body, down to the temperature of isotopic closure for Nd and Sr has been estimated to be roughly 100 m.y. (Warren et al. 1991). Such very early shocks have been suggested for other diogenites and eucrites using radiochronological studies (e.g., Bogard et al. 1992; Kunz et al. 1995; Yamaguchi et al. 1997). A high pre-shock temperature has also been proposed for the Johnstown diogenite based on mineralogical arguments (Mori and Takeda 1981).

ACKNOWLEDGMENTS

Adrian Brearley and two anonymous reviewers are acknowledged for detailed and constructive criticisms about an early version of this work, which led to strong improvements of this paper.

REFERENCES CITED

- Barrat, J.A., Gillet, Ph., Lécuyer, C., Sheppard, S.M.F., and Lesourd, M. (1998) Formation of carbonates in the Tatahouine meteorite. *Science*, 280, 412–414.
- Barrat, J.A., Gillet, Ph., Lesourd, M., Blichert-Toft, J., and Poupeau, G.R. (1999) The Tatahouine diogenite: Mineralogical and chemical effects of sixty-three years of terrestrial residence. *Meteoritics and Planetary Science*, 34, 91–97.
- Binzel, R.P. and Xu, S. (1993) Chips off Asteroid 4 Vesta: Evidence for the parent body of basaltic achondrite meteorites. *Science*, 260, 186–191.
- Bischoff, A. and Stöfler, D. (1992) Shock metamorphism as a fundamental process in the evolution of planetary bodies: information from meteorites. *European Journal of Mineralogy*, 4, 707–755.
- Bogard, D., Nyquist, L., Takeda, H., Mori, H., Bansal, B., Wiesmann, H., and Shih, C.-Y. (1992) Antarctic polymict eucrite Yamato 792769 and the cratering record on the HED parent body. *Geochimica et Cosmochimica Acta*, 57, 2111–2121.
- Brett, R. (1976) Reduction of mare basalts by sulfur loss. *Geochimica et Cosmochimica Acta*, 40, 997–1004.
- Buseck, P.R., Nord, G.L., and Veblen, D.R. (1980) Subsolidus phenomena in pyroxenes. In C.T. Prewitt, Ed., *Pyroxenes*, p. 117–211. *Reviews in Mineralogy*, Mineralogical Society of America, Washington, D.C.
- Champness, P.E. (1970) Nucleation and growth of iron oxides in olivines, (Mg,Fe)₂SiO₄. *Mineralogical Magazine*, 37, 790–800.
- Chen, M. and El Goresy, A. (2000) The nature of maskelynite in shocked meteorites: not diaplectic glass but a glass quenched from shock-induced dense melt at high pressures. *Earth Planetary Science Letters*, 179, 489–502.
- Clayton, R.N. and Mayeda, T.K. (1996) Oxygen isotope studies of achondrites. *Geochimica et Cosmochimica Acta*, 60, 1999–2017.
- Coe, R.S. and Kirby, S.H. (1975) The orthoenstatite to clinoenstatite transformation by shearing and reversion by annealing: Mechanism and potential applications. *Contributions to Mineralogy and Petrology*, 52, 29–55.
- Doukhan, J.-C., Doukhan, N., Nazé, L., and Van-Duyssens, J.C. (1986) Défauts de réseau et plasticité cristalline dans les pyroxènes: Une revue. *Bulletin de Minéralogie*, 109, 377–394.
- Doukhan, N. and Doukhan, J.-C. (1993) Early partial melting in pyroxenes. *American Mineralogist*, 78, 1246–1256.
- Drake, M.J. (1979) Geochemical evolution of the eucrite parent body: Possible nature and evolution of asteroid 4 Vesta? In T. Gehrels, Ed., *Asteroids*, p. 765–782. Univ. Arizona Press, Tucson.
- El Goresy, A., Dubrovinsky, L., Sharp, T.G., Saxena, S.K., and Chen, M. (2000) A monoclinic post-stishovite polymorph of silica in the Shergotty meteorite. *Science*, 288, 1632–1634.
- Fowler, G.W., Papke, J.J., Spilde, M.N., and Shearer, C.K. (1994) Diogenites as asteroid cumulates: Insights from orthopyroxene trace elements chemistry. *Geochimica et Cosmochimica Acta*, 59, 3071–3084.
- Fredriksson, K., Noonan, A., Brenner, P., and Sudre, C. (1976) Bulk and major phase composition of eight hypersthene achondrites. *Meteoritics*, 11, 278–280.
- Frondele, C. (1962) *The System of Mineralogy, Silica Minerals*. System of Mineralogy, vol. III: Silica Minerals. J. Wiley and Sons, New York.
- Gibbons, R.V. and Ahrens, T.J. (1971). Shock metamorphism of silicate glasses. *Journal of Geophysical Research*, 76, 5489–5498.
- Gillet, Ph., Le Cléach, A., and Madon, M. (1990) High-temperature Raman spectroscopy of the SiO₂ and GeO₂ polymorphs: anharmonicity and thermodynamic properties at high-temperature. *Journal of Geophysical Research*, 95, 21635–21655.
- Gillet, Ph., Barrat, J.A., Heulin, Th., Achouak, W., Lesourd, M., Guyot, F., and Benzerara, K. (2000a) Bacteria in the Tatahouine meteorite: nanometric-scale life in rocks. *Earth and Planetary Science Letters*, 175, 161–167.
- Gillet, Ph., Chen, M., Dubrovinsky, L., and El Goresy, A. (2000b) Natural NaAlSi₃O₈-hollandite in the shocked Sixiangkou meteorite. *Science*, 287, 1633–1636.
- Gooley, R. and Moore, C.B. (1976) Native metal in diogenite meteorites. *American Mineralogist*, 61, 373–378.
- Gratz, A.J., De Loach, L.D., Clough, T.M., and Nellis, W.J. (1993) Shock amphibization of cristobalite. *Science*, 259, 663–666.
- Greshake, A., Stephan, T., and Rost, D. (1998) Symplectic exsolutions in olivine from the martian meteorite Chassigny: Evidence for slow cooling under highly oxidizing conditions. *LPSC XXIX*, 1069.
- Kondoh, S., Kitamura, M., and Morimoto, N. (1985) Synthetic laihunite, an oxidation product of olivine. *American Mineralogist*, 70, 737–746.
- Kunz, J., Trieloff, M., Bobe, K.D., Metzler, K., Stöfler, D., and Jessberger, E.K. (1995) The collisional history of the HED parent body inferred from ⁴⁰Ar-³⁹Ar ages of eucrites. *Planetary Space Science*, 43, 527–543.
- Lacroix, A. (1931) Sur la chute récente (27 Juin 1931) d'une météorite asidérite dans l'Extrême Sud tunisien. *Comptes Rendus de l'Académie des Sciences, Paris*, 193, 305–309.
- (1932) La météorite (diogénite) de Tatahouine, Tunisie (27 Juin 1931). *Bulletin de la Société Française de Minéralogie*, 55, 101–122.
- Lovering, J.F. (1975) The Moama eucrite-a pyroxene-plagioclase adcumulate. *Meteoritics*, 10, 101–114.
- Lugmair, G.W. and Shukolyukov, A. (1998) Early solar system timescales according to ⁵³Mn-⁵³Cr systematics. *Geochimica et Cosmochimica Acta*, 62, 2863–2886.
- Malavergne, V., Guyot, F., Benzerara, K., and Martinez, I. (2001) Description of new shock-induced phases in the meteorites of Shergotty, Zagami, Nakhla and Chassigny. *Meteoritics and Planetary Science*, 36, 1297–1305.
- Martinez, I., Schärer, U., Ildefonso, P., Guyot, F., and Agrinier, P. (1993) Impact-induced phase transformations at 50–60 GPa in continental crust: an EPMA and ATEM study. *Earth Planetary Science Letters*, 119, 207–223.
- Mittlefehldt, D.W. (1994) The genesis of diogenites and HED parent body petrogenesis. *Geochimica et Cosmochimica Acta*, 58, 1537–1552.
- Mori, H. and Takeda, H. (1981) Thermal and deformational histories of diogenites as inferred from their microtextures of orthopyroxene. *Earth and Planetary Let-*

- ters, 53, 266–274.
- Nord, G.L. and Hewins, R.H. (1983) Thermal and mechanical history of Tatahouine diogenite. *Meteoritics*, 18, 364–365.
- Palme, H., Wlotzka, F., Spettel, B., Dreibus, G., and Weber, H. (1988) Camel Donga: a eucrite with high metal content. *Meteoritics*, 23, 49–57.
- Palmer, D.C., Hemley, R.J., and Prewitt, C.T. (1994) Raman spectroscopic study of high-pressure phase transitions in cristobalite. *Physics and Chemistry of Minerals* 21(8), 481–488.
- Papike, J.J., Spilde, M.N., Fowler, G.J., and Shearer, C.K. (1995) The Lodran primitive achondrite: petrogenetic insights from electron and ion microprobe analyses of olivine and orthopyroxene. *Geochimica et Cosmochimica Acta*, 59, 3061–3070.
- Papike, J.J., Shearer, C.K., Spilde, M.N., and Karner, J.M. (2000) Metamorphic diogenite GRO9555: mineral chemistry of orthopyroxene and spinel and comparisons to diogenite suite. *Meteoritics and Planetary Sciences*, 35, 875–879.
- Rehfeldt, A., Oskierski, A., Stöffler, D., and Hornemann, U. (1986) Deformation, transformation and thermal annealing of experimentally shocked single crystal quartz (abstract). *Lunar Planetary Sciences XVII*, 697–698.
- Richet, P., and Gillet, P. (1997) Pressure-induced amorphization of minerals: a review. *European Journal of Mineralogy*, 9, 907–933.
- Rubin, A.E., Scott, E.R.D., and Keil, K. (1997) Shock metamorphism of enstatite chondrites. *Geochimica et Cosmochimica Acta*, 61, 845–858.
- Sharma, S.K. (1989) Applications of advanced Raman techniques in Earth sciences. In H.D. Bist, J.R. Durig, and J.F. Sullivan, Eds., *Raman Spectroscopy: Sixty Years On, Vibrational Spectra and Structure*, p 513–568. Elsevier, Amsterdam.
- Stöffler, D. (1982) Density of minerals and rocks under shock compression. In K.–H. Hellwege, Ed., *Landolt-Börnstein-numerical data and functional relationships in science and technology*, Vol. 1, p. 120–183. Physical Properties of Rocks, Springer Verlag, Berlin.
- Stöffler, D., Keil, K., and Scott, E.R.D. (1991) Shock metamorphism of ordinary chondrites. *Geochimica et Cosmochimica Acta*, 55, 3845–3867.
- Thiéblot, L., Téquie, C., and Richet, P. (1999) High-temperature heat capacity of grossular ($\text{Ca}_3\text{Al}_2\text{Si}_3\text{O}_{12}$), enstatite (MgSiO_3), and titanite (CaTiSiO_5). *American Mineralogist*, 84, 848–855.
- Tsuchida, Y. and Yagi, T. (1990) New pressure-induced transformations of silica at room temperature. *Nature*, 347, 267–269.
- Warren, P.H. (1997) Magnesium oxide-iron oxide mass balance constraints and a more detailed model for the relationship between eucrites and diogenites. *Meteoritics and Planetary Sciences*, 32, 945–963.
- Warren, P.H., Haack, H., and Rasmussen, K.L. (1991) Megaregolith insulation and the duration of cooling to isotopic differentiated asteroids and the moon. *Journal of Geophysical Research*, 96, 5909–5923.
- Weber, I., Greshake, A., and Bischoff, A. (2000) Low cristobalite in the martian meteorite Zagami. *LPSC XXXI*, 1342.
- Withers R.L., Thompson J.G., and Welberry T.R. (1989) The structure and microstructure of α -cristobalite and its relationship to β -cristobalite. *Physics and Chemistry of Minerals*, 16, 517–523.
- Yamaguchi, A., Taylor, G.J., Keil, K., and Bogard, D.D. (1997) Evidence for a large cratering event on the HED parent body (Vesta) ~4.5 Ga ago. *Meteoritics and Planetary Science*, 32, A144–A145.
- Zhang, X. and Ong, C.K. (1993) Pressure-induced amorphization of β -cristobalite. *Physical Review B*, 48, 6865–6870.

MANUSCRIPT RECEIVED MAY 21, 2001

MANUSCRIPT ACCEPTED MAY 16, 2002

MANUSCRIPT HANDLED BY ADRIAN J. BREARLEY